ACS APPLIED MATERIALS & INTERFACES

Research Article

www.acsami.org

Immunochromatographic Assay for Ultrasensitive Detection of Aflatoxin B_1 in Maize by Highly Luminescent Quantum Dot Beads

Meiling Ren,[†,‡,∥] Hengyi Xu,[†,∥] Xiaolin Huang,[†,‡] Min Kuang,[§] Yonghua Xiong,*[,†,‡] Hong Xu,[§] Yang Xu,[†,∥] Hongyu Chen,[§] and Andrew Wang*[,§]

[†]State Key Laboratory of Food Science and Technology, Nanchang University, Nanchang 330047, People's Republic of China

[‡]Jiangxi-OAI Joint Research Institute, Nanchang University, Nanchang 330047, People's Republic of China

[§]Ocean NanoTech, LLC, San Diego, California 92126, United States

Supporting Information

ABSTRACT: Highly luminescent quantum dot beads (QBs) were synthesized by encapsulating CdSe/ZnS and used for the first time as immunochromatographic assay (ICA) signal amplification probe for ultrasensitive detection of aflatoxin B_1 (AFB_1) in maize. The challenges to using high brightness QBs as probes for ICA are smooth flow of QBs and nonspecific binding on nitrocellulose (NC) membrane, which are overcome by unique polymer encapsulation of quantum dots (QDs) and surface blocking method. Under optimal conditions, the QB-based ICA (QB-ICA) sensor exhibited dynamic linear detection of AFB_1 in maize extract from 5 to 60 pg mL^{-1}, with a median inhibitory concentration (IC_{50}) of 13.87 ± 0.16 pg mL^{-1}, that is significantly (39-fold) lower than those of the QD as a signal probe (IC_{50} = 0.54 ± 0.06 ng mL^{-1}). The limit of detection (LOD) for AFB_1 using QB-ICA sensor was 0.42 pg mL^{-1} in maize extract, which is approximately 2 orders of magnitude better than those of previously reported gold nanoparticle based immunochromatographic assay (AuNP-ICA) and is even comparable with or better than the conventional enzyme-linked immunosorbent assay (ELISA) method. The performance and practicability of our QB-ICA sensor were validated with a commercial ELISA kit and further confirmed with liquid chromatography tandem mass spectrometry (LC−MS/MS). Given its efficient signal amplification performance, the proposed QB-ICA offers great potential for rapid, sensitive, and cost-effective quantitative detection of analytes in food safety monitoring.

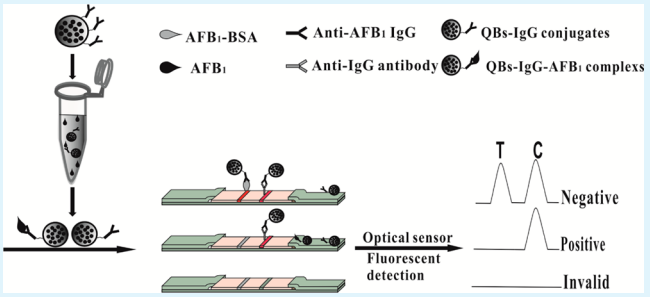

KEYWORDS: *quantum dot, beads, immunochromatographic assay, quantitative detection, aflatoxin B_1*

1. INTRODUCTION

Aflatoxin B_1 (AFB_1) is one of the most compelling mycotoxins and is listed as a Group I carcinogen by the International Agency for Research in Cancer.[1] Many countries have established regulations to govern the AFB_1 level in agricultural products to avoid overexposure of humans and animals to AFB_1.[2] The Ministry of Agriculture of China has set up the maximum allowed level (MAL) in foodstuffs at 20 ng mL^{-1}. The European Union has established a lower MAL of AFB_1 in groundnuts, milk, dried fruits, and cereals, as well as their products, at 2 ng mL^{-1}.

Various immunochemical methods, including enzyme-linked immunosorbent assay (ELISA),[3,4] microarray,[5] and other immunobiosensors, have been developed for highly sensitive detection of AFB_1 because of their specificity and reliability. For example, Yu et al. reported a direct competitive chemiluminescent ELISA for determination of AFB_1 with a limit of detection (LOD) of 1.5 pg mL^{-1}.[6] Hu et al. developed a nonfouling polymer brush-based fluorescent competitive immunoassay microarray to detect multiplex mycotoxins, including AFB_1 with an LOD of 4 pg mL^{-1}.[7] Deng et al. reported an ultrasensitive immunoassay using silica photonic crystal microsphere suspension array method for multiplex mycotoxin detection with an LOD at 0.5 pg mL^{-1} for AFB_1.[8] However, these immunochemical methods require both professional laboratory conditions and skilled operators. These methods are also time-consuming because they have complex handling procedures; thus, they are unsuitable for on-site rapid screening detection of AFB_1.

Recently, gold nanoparticle based immunochromatographic assay (AuNP-ICA) has been applied extensively to detect AFB_1 because of its significant potential advantages over conventional laboratory-based testing technologies, such as simplicity, rapidity, portability, low cost, and ease of use and maintenance.[9−13] Zhang et al. reported an ultrasensitive AuNP-ICA to detect total aflatoxins, and the visual LOD was achieved at 30 pg mL^{-1}.[14] However, AuNP-ICA lacks sensitivity comparisons with conventional ELISA and micro-

Received: June 4, 2014
Accepted: August 9, 2014
Published: August 9, 2014

Scheme 1. Procedure for the Detection of AFB_1 Using QBs

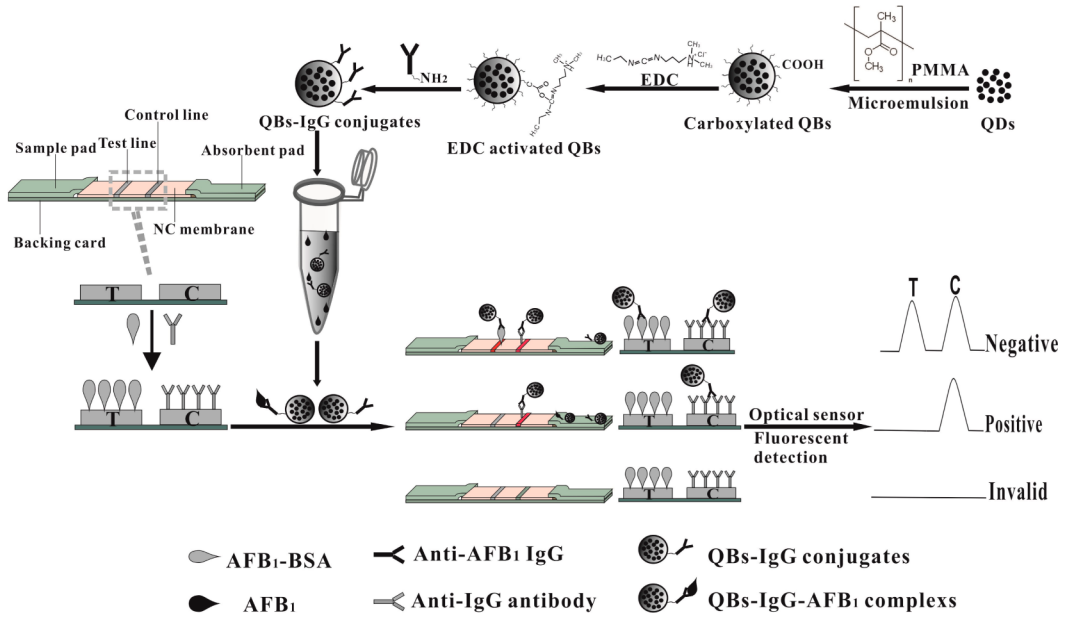

array methods. Several alternative labels, including colloidal carbon,[15] magnetic nanoparticles,[16] up-converting phosphors,[17] time-resolved fluorescence,[18] quantum dots (QDs),[19] and organic or inorganic dye-doped nanoparticles,[20] have been utilized to improve the detection sensitivity of ICA. Among these novel labels, QDs are one of the ideal fluorescent labels because of their broad UV excitation, narrow fluorescent emission spectra, high quantum yield, large molar extinction coefficient, and high photostability.[21,22] Theoretically, doping or encapsulating numerous QDs on or inside polybeads may improve the sensitivity of ICA by amplifying the detectable signal of the recognition events. Zhang et al. developed a quantum dots nanobeads based dot-blot immunoassay for ultrasensitive detection of hepatitis B virus surface antigen with an LOD of 0.078 ng mL^{-1}.[23] Yuan et al. reported a layer-by-layer assembly of QDs as a signal simplification label for ultrasensitive electronic detection of uropathogens, with an LOD of 0.22 fmol.[24] Meanwhile, Li et al. also reported an application of QD nanobeads for detection of prostate specific antigen based on a sandwich ICA sensor.[25] However, QD-doped or encapsulated beads as an amplification label for competitive ICA sensor has not been reported.

In the current study, highly luminescent submicrobeads were synthesized by encapsulating CdSe/ZnS QDs using the microemulsion technique. The resultant QD encapsulated submicrobeads (QBs) exhibited approximately 2863 times brighter luminescence than the corresponding QDs. The QBs were proposed for the first time as an ICA signal amplification probe for ultrasensitive detection of AFB_1 in maize. A homemade portable strip reader was used to record fluorescence intensity (FI) on the test line (FI_T) and control line (FI_C) for possible on-site quantitative detection of AFB_1 in maize within 15 min. The sensitivity of QB-based ICA (QB-ICA) shows approximately 2 orders of magnitude higher than those of previously reported AuNP-ICA because of the thousands of CdSe/ZnS QDs contained in a single QB. Additionally, QB-ICA is comparable or even superior to conventional ELISA or microarray methods. Hence, the QB-ICA sensor offers great potential for rapid, sensitive, and cost-effective quantitative detection of analytes in food safety monitoring.

2. MATERIALS AND METHODS

2.1. Materials and Reagents. *N*-(3-(Dimethylamino)propyl)-*N*′-ethylcarbodiimide hydrochloride (EDC·HCl), AFB_1, and bovine serum albumin (BSA) were purchased from Sigma-Aldrich Chemical (St. Louis, MO). AFB_1–BSA conjugates (mole ratio of 15:1) and anti-AFB_1 mAbs were prepared in our laboratory. Donkey anti-mouse IgG antibodies were purchased from Beijing Zhongshan Biotechnology, Inc. (Beijing, China). The sample pad, nitrocellulose (NC) membrane, and absorbent pad were obtained from Schleicher and Schuell GmbH (Dassel, Germany). The commercial AFB_1 ELISA kit was provided by Wuxi Zodoboer Biotech. Co., Ltd. (Wuxi, China). The phosphate-buffered saline (PBS, 0.01 M, pH 7.4) was obtained by adding 1.22 g of K_2HPO_4, 1.36 g of KH_2PO_4, and 8.5 g of NaCl in 1000 mL of Milli-Q water and adjusted to 7.4, unless otherwise specified, before use. All of the other reagents were of analytical grade or better and purchased from Sinopharm Chemical Corp. (Shanghai, China).

2.2. Apparatus. The BioDot XYZ platform combined with a motion controller, BioJet Quanti3000k dispenser, and AirJet Quanti3000k dispenser for solution dispensing, were supplied by BioDot (Irvine, CA). An automatic programmable cutter was purchased from Shanghai Jinbiao Biotechnology Co., Ltd. (Shanghai, China). Pure water used for all the experiments was purified by Elix-3 and Milli-QA (Molsheim, France).

2.3. Preparation of QBs. CdSe/ZnS QDs were prepared according to a previously reported method.[26] The QBs were prepared by applying a microemulsion technique. Briefly, 20 mg of CdSe/ZnS QDs were dissolved with 2 mL of $CHCl_3$ containing 60 mg mL^{-1} of poly(methyl methacrylate) (PMMA) and 40 mg mL^{-1} of poly(maleic anhydride-*alt*-1-octadecene) (PMAO), and then mixed with 5 mL of sodium dodecyl sulfonate aqueous solution (3 mg mL^{-1}). The mixture emulsion was obtained using an ultrasonic homogenizer for 2 min. The nonpolar solvent ($CHCl_3$) was evaporated by a Rotovap R-200 (Buchi U.K. Ltd., Oldham, U.K.). The resulting water-soluble QBs were purified by centrifugation (10 000 rpm, 10 min) and washed thrice with pure water. The size distribution and morphology of the QBs were characterized by a high-resolution scanning electron microscope (Hitachi S-4800, Tokyo, Japan) and a high-resolution transmission electron microscope (JEOL JEM 2100, Tokyo, Japan). The photoluminescence spectrum of the QBs was recorded by a fluorescence spectrophotometer (Hitachi F-4500, Tokyo, Japan).

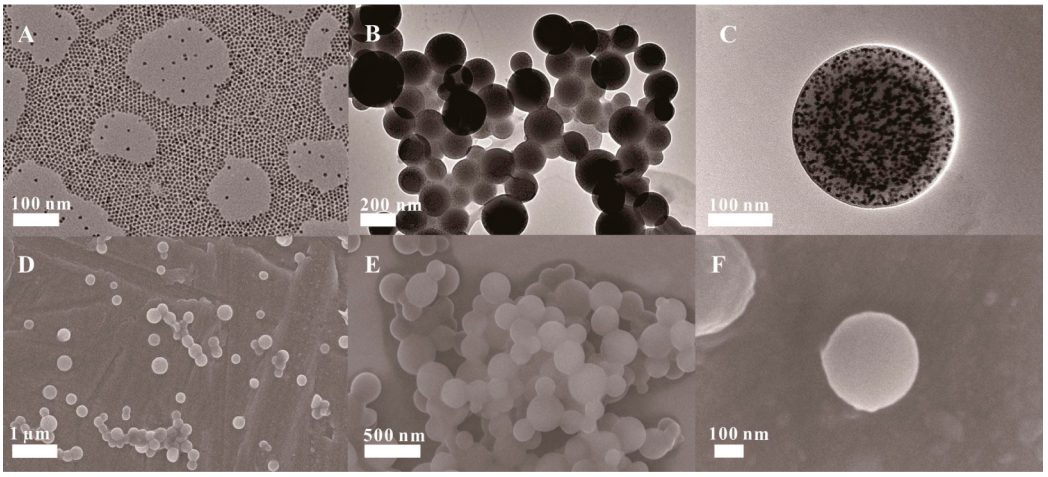

Figure 1. TEM image of (A) CdSe/ZnS QDs in QBs and of (B and C) QBs with different magnifications. (D−F) SEM images of QDs with different magnifications.

2.4. Preparation of the QB-mAbs. The ascetic fluid containing 4% anti-AFB_1 mAbs was conjugated to QBs directly, as previously described with some modifications.[27] Briefly, 1.0 μg of EDC and 0.12 mg of QBs were added to 2.7 mL of 0.01 M phosphate buffer (pH 6.0), and then the desired concentration of the ascetic fluid was added dropwise to the EDC-activated QBs under gentle stirring. The mixture reacted at room temperature for 40 min. Subsequently, the QB-mAbs were separated by centrifugation at 13 500g for 10 min, and then the precipitates were resuspended with 600 μL of PBS (0.01 M, pH 7.4) containing 5% sucrose, 2% fructose, 1% PEG 20000, 1% BSA, and 0.4% Tween-20. The resuspended solution was stored at 4 °C for further use. To confirm the immobilization of the anti-AFB_1 mAbs on the surface of QBs, the free QBs and QB-mAbs probes were characterized with a particle size analyzer (Malvern Instruments Ltd., Worcestershire, U.K.) and Nicolet5700 FTIR spectroscopy (Thermo Fisher Scientific, Inc., Waltham, MA), respectively.

2.5. Fabrication of QB-ICA Sensor. The formation and principle of the QB-ICA sensor are shown in Scheme 1. The test strip comprised three parts: sample pad, NC membrane, and absorbent pad. The sample pads were saturated with 20 mmol L^{-1} sodium borate buffer (pH 8.0), containing 1.0% (w/v) BSA, 0.25% Tween-20, and 0.1% (w/v) NaN_3, and dried at 60 °C for 2 h. The AFB_1−BSA (0.4 mg mL^{-1}) and donkey anti-mouse IgG antibodies (1 mg mL^{-1}) were dispensed onto the NC membrane as test and control lines at densities of 4 μL cm^{-1}, respectively, and then dried at 37 °C for 4 h. The sample pad, NC membrane, and absorbent pad were assembled onto a backing card overlapping 2 mm on top of each other. The assembled backing card was cut into 4 mm wide strip using an automatic programmable cutter, sealed in a plastic bag with desiccant gel, and stored at room temperature until use.

2.6. Quantitative Procedure of QB-ICA Sensor. Approximately 5.0 μL of QB-mAbs probe (36 μg mL^{-1}) and 75 μL of sample solution were premixed at room temperature and then added into the well of the sample pad. After a 15 min incubation period, the strip was scanned with an optical reader, which was provided by Shanghai Huguo Science Instrument Co., Ltd. (Shanghai, China). FI_T, FI_C, and FI_T/FI_C were recorded. The AFB_1 quantitative analysis was calculated according to a linear regression equation of the AFB_1 calibration curve. The standard curve was established by plotting the $B/B_0 \times 100\%$ against the logarithm of the AFB_1 concentration, where B and B_0 represented FI_T/FI_C, with and without the presence of competitive antigen (AFB_1) in the standard solutions. The standard AFB_1 solutions were prepared by spiked stock AFB_1 solution (20 ng mL^{-1}) in PBS containing 3.0% methanol (v/v) at pH 7.4 to a final concentration of 0 (as negative control), 0.25, 0.5, 1.0, 2.0, 5.0, 10, 15, 20, 30, 40, 60, 100, 150, and 200 pg mL^{-1}.

2.7. Spiked Maize Samples. The 46 maize samples (N = 46), which were confirmed to be free of AFB_1 by LC−MS/MS, were collected from the grain procurement agencies in Jining and Shandong Provinces in China. All samples were ground prior to AFB_1 extraction, and the sample extracts used for the ICA assay were prepared as follows: 5.0 g of the pulverized sample was extracted with 25 mL methanol−water (70:30, v/v) for 20 min on a vortex shaker. After centrifugation at 12 000g for 10 min, the supernatant solutions were stored at −20 °C and further diluted 60-fold with PBS (0.01 M, pH 7.4) buffer before QB-ICA analysis. Three spiked maize extracts with AFB_1 concentrations of 10, 20, and 40 pg mL^{-1} were prepared for accuracy and precision analysis.

2.8. Comparative Evaluation with Commercial ELISA Kit. Up to 40 random blank maize samples, which were spiked AFB_1 concentrations over the range of 0.5−9.0 ng g^{-1}, were determined using the QB-ICA sensor and commercial AFB_1 ELISA kit. Sample pretreatment for the commercial ELISA kit was performed according to the manufacturer's instructions.

2.9. LC−MS/MS Analysis. The reliability and practicability of QB-ICA sensor was further confirmed by a triple quadrupole LC−MS/MS system (Agilent Technologies, Lexington, MA), which was composed of triple quad instrument (Agilent 6410) and LC system (Agilent 1200 series). Nine different feedstuff materials, including maize, soybean meal, rapeseed meal, cotton seed meal, distillers dried grain, and wheat sample were provided by Jiangxi Institute of Veterinary Drug and Feedstuff Control (Nanchang, China). The sample extraction, cleanup, and LC−MS/MS operation were performed according to the local standard GB/T 22286-2008 (Sichuan, China) with some modifications. Pulverized sample (5.0 g) was extracted with 25 mL methanol−water (70:30, v/v) for 40 min on a vortex shaker. After centrifugation at 10 000g for 10 min, 3 mL of the supernatant solutions were further diluted 4-fold with 9 mL PBS (0.01 M, pH 7.4) and then cleaned using immune affinity column provided by Beijing Rapid Bioscience Co., Ltd. (Beijing, China). The purified AFB_1 solution was filtered with a 0.22 μm cellulose membrane and further used for LC−MS/MS analysis. The LC−MS/MS system was controlled by MassHunter software (Agilent Technologies, Lexington, MA). The chromatographic separation was performed with Agilent Zorbax Eclipse XDB-C18 column (250 mm × 4.6 mm, 5 μm) that was maintained at 30 °C. The mobile phase consisted of solvent A (ammonium acetate, 10 mM) and solvent B (methanol). Initial gradient conditions were set at 80% solvent A, reduced with a linear gradient to 15% from 0 to 6.0 min, and then reduced to 5% from 6.0 to 8.0 min. At 8.0 min, the gradient was programmed to initial conditions to re-equilibrate the column for 4.0 min. The flow rate was 0.30 mL min^{-1}, and the injection volume was 5 μL in full loop injection mode. Ionization was achieved using electrospray ionization in positive ion mode. Detection was conducted in multiple reaction monitoring mode. High-purity nitrogen gas was used for desolvation, cone, and collision gas. The monitoring ion pairs

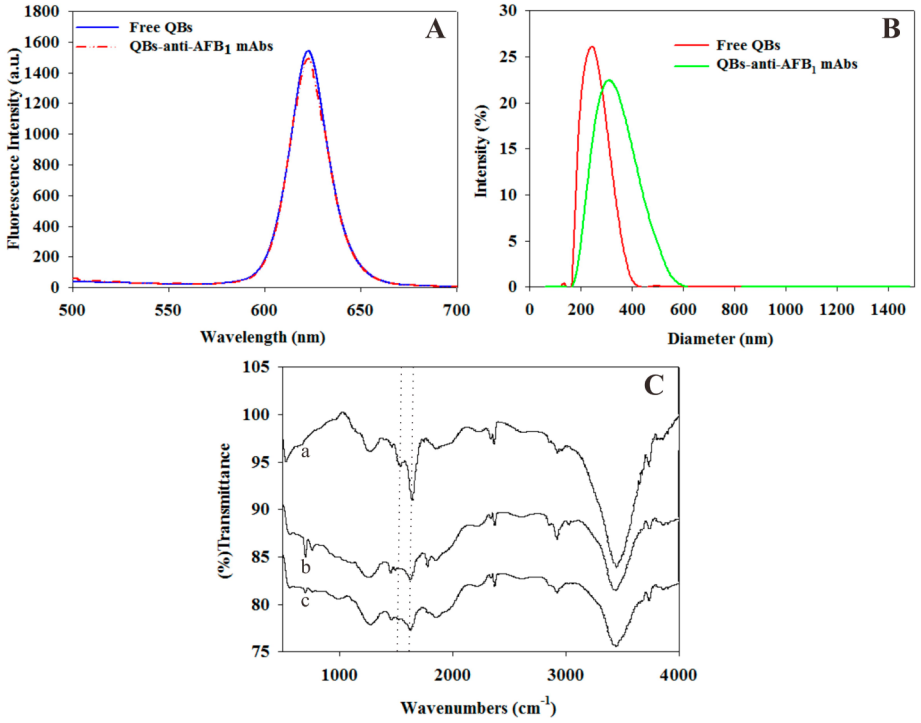

Figure 2. Characterization of the free QBs and QB-mAbs conjugates. (A) Fluorescence spectra of QBs and QB-mAbs conjugates in the same concentration (7.99 pmol L^{-1}). (B) Hydrodynamic diameter of QBs and QB-mAbs. (C) FTIR spectra of (curve a) anti-AFB_1 ascites, (curve b) QBs, and (curve c) QB-mAbs.

were chosen as AFB_1 m/z 313.1/285.1 (quantitation ion) and 313.1/241.1 (qualitative ions).

3. RESULTS AND DISCUSSION

3.1. Characterization of QBs and Anti-AFB_1 mAbs QB Probe. Highly luminescent CdSe/ZnS QDs were initially prepared to fabricate QBs based on a modified method reported by Xie et al.[26] The as-prepared QDs were monodispersed with an average size of 8.5 ± 1 nm (Figure 1A). The absorption and fluorescence spectra of the core/shell nanocrystals are presented in Figure S1 (Supporting Information). The narrow features of the emission peaks are consistent with the narrow size distribution of the core/shell nanocrystals shown in Figure 1A. Modified microemulsion based on poly(methyl methacrylate) (PMMA) and poly(maleic anhydride-*alt*-1-octadecene) (PMAO) composites was used to encapsulate numerous single QDs in a polymer matrix. The size and morphology of the prepared QBs were studied under a high-resolution transmission electron microscope (TEM) and a scanning electron microscope (SEM). High-resolution TEM images (Figure 1B,C) show a compact QD-polymer structure, indicating that the numerous, individual dark dots with a diameter of approximately 8.5 nm are tightly encapsulated in the polymer matrix. These dark dots are QDs, which can be visibly identified from the polymer matrix because of the different electron penetrabilities between the QDs and polymer matrix. The typical SEM images of the QBs in Figure 1D−F show that the obtained QBs are well distributed and relatively uniform spherical submicrobeads. The histogram of size distribution indicates that the submicrobeads have an average diameter of 247 ± 13 nm (Figure S2, Supporting Information). The fluorescence spectrum of QBs also presents a bright and narrow fluorescence peak at 620 nm, with full width at half-maximum of 25 nm. This emission peak is in the same position as the single QDs but with an enhanced intensity approximately 2863 times brighter than the corresponding QDs. A detailed calculation is presented in Figure S3 (Supporting Information). All these optical characteristics of the QBs suggest that our microemulsion-based method to prepare QBs is excellent at maintaining the characteristics of QDs. Thus, the strong fluorescence signal of the prepared QBs provides a promising platform to improve the analytical sensitivity of ICA sensor. Meanwhile, the stable polymer matrix prevents the leakage of trapped QDs into the surrounding environment, which minimizes photobleaching and photodegradation.[28]

The anti-AFB_1 mAbs-labeled QB probes (QB-mAbs) were prepared by coupling the amino group of anti-AFB_1 ascites with the carboxyl group of the QBs using the active ester method.[29] Photoluminescence spectrophotometer, particle size analyzer, and Fourier-transform infrared (FTIR) spectroscopy were utilized to characterize the free QBs and QB-mAbs. The fluorescence spectra showed that after the conjugation, the FI of QB-mAbs slightly decreased compared with free QBs (Figure 2A). The average hydrodynamic diameter of QB-mAbs increased from 255 ± 3 nm (free QBs) to 295 ± 5 nm after the anti-AFB_1 ascites conjugated on the surface of QBs (Figure 2B). To confirm the immobilization of anti-AFB_1 ascites on the surface of QBs, FTIR analyses of QB-mAbs were performed, and results were compared with those of free QBs and anti-AFB_1 ascites. Compared with those of the free QBs (Figure 2C, curve b), the FTIR spectra of the anti-AFB_1 ascites and QB-mAbs showed that characteristic absorption peaks corresponding to protein amide bands I (1641 cm^{-1}) and II (1530 cm^{-1}), respectively (Figure 2C, curves a and c). The anti-AFB_1 ascites were successfully covalently bound on the surface of the QBs.

3.2. Optimization of the Saturated Labeled Ascites on the QBs. The unpurified anti-AFB_1 ascites were used to conjugate with the QBs directly. Prior to conjugation, the

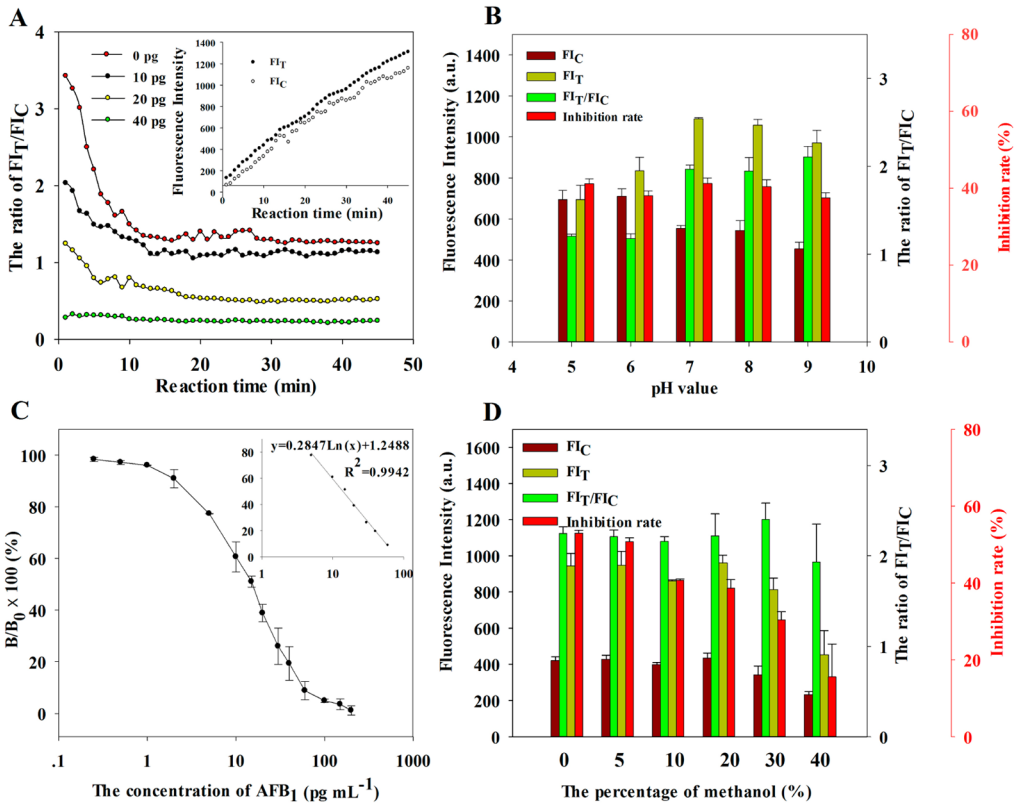

Figure 3. (A) Immunoreaction dynamics of FI_T/FI_C at different AFB_1 concentrations. (B) Effect of pH value of samples on FI_T, FI_C, and FI_T/FI_C ratio. Competitive inhibition rate was defined as $(1 - B/B_0) \times 100\%$, where B_0 and B represent FI_T/FI_C of the negative sample and an AFB_1 spiked sample solution (10 pg mL^{-1}), respectively. (C) Optimized standard inhibition curve for AFB_1 was obtained by plotting the normalized signal $B/B_0 \times 100\%$ against the logarithm of AFB_1 concentration. Data were obtained by averaging three independent experiments. (D) Effect of methanol in samples on FI_T, FI_C, and FI_T/FI_C ratio.

unpurified anti-AFB_1 ascites were verified by the target antibody (4%) and miscellaneous protein (96%), as shown in Figure S4 (Supporting Information). Along with the conjugation process, the desired antibody could be coupled with the carboxyl group of the QBs, whereas the mass of the miscellaneous protein blocked the excess carboxyl groups of the QBs to reduce the nonspecific binding of the QBs with NC membrane and the antigen on the test line. To estimate the saturated labeling content of protein on the surface of the QBs, 1 mg of QBs was conjugated with a series amount of anti-AFB_1 ascites from 10 to 300 μg. The resultant QB-mAbs were then run on the ICA sensor, and the fluorescent signal was recorded using a portable strip reader. Figure S5 (Supporting Information) shows that FI_T increased from 180.08 ± 3.82 to 1100.21 ± 68.00, and the content of the labeled ascites increased from 10 to 150 μg per mg of the QBs. Then, the FI became saturated as the ascites contents increased. Therefore, 150 μg of ascites per mg of QBs was verified as the saturated labeled concentration.

3.3. Optimization of the QB-ICA Sensor. In a traditional strip, the labeled probes are dispensed or sprayed on the conjugated pad, and they may diffuse in an irregular manner along the glass fiber, which might easily lead to nonreproducibility between the different strips and affect the sensitivity of the assay.[14] In the present study, the conjugated pad was omitted, and the new strip was assembled by overlapping 2 mm of the sample pad, NC membrane, and absorbent pad on top of each other on the backing card, as illustrated in Scheme 1. The QB-mAbs were premixed with the sample solution before performing the test as a previously described protocol.[30] Compared with the traditional strip, the FI_T value of the new strip improved from 751.08 to 1057.34, whereas the FI_C value increased from 390.92 to 559.74. Meanwhile, the coefficient of variation (CV) of FI_T/FI_C between the different strips (N = 10) decreased from 15.34 to 7.0%.

To achieve the best sensitivity and a higher FI signal on both lines, a similar "checkerboard titration" was performed with different QB-mAbs contents under a series of AFB_1–BSA conjugates on the test line for various combinations. The competitive inhibition rates and FI signals on both lines are used to confirm the optimal parameters, from which the competitive inhibition rates are obtained by $(1 - B/B_0) \times 100\%$, where B_0 and B represent FI_T/FI_C of the negative sample and an AFB_1-spiked maize extract sample (10 pg mL^{-1}), respectively. Table S1 (Supporting Information) presents the results, which indicated the following optimal combinations: 0.4 mg mL^{-1} AFB_1–BSA was spotted on the NC membrane as the test line, and 150 μg of anti-AFB_1 ascites was used to conjugate with 1 mg of QBs and 5 μL of QB-mAbs probe (36 μg mL^{-1}) were premixed with 75 μL sample solution. Under the optimized parameters, the competitive inhibition rate of the ICA sensor for a 10 pg mL^{-1} AFB_1 sample was achieved at 40.16%, the FIs on the test and control lines were 1221.49 and 633.97, respectively, which could be observed on the strong red fluorescence bands on the test and control zones under an ultraviolet (UV) lamp excitation. The stereogram of the strip is displayed in Figure S6 (Supporting Information).

Table 1. Precision and Stability of the Test Strip in AFB_1-Spiked Samples

	intra-assay				inter-assay[a]			
spiked AFB_1 (pg mL^{-1})	mean[b]	recovery (%)	SD	CV (%)	mean[b]	recovery (%)	SD	CV (%)
40	39.15	97.89	2.70	6.89	38.52	96.32	3.68	5.57
20	20.21	101.05	0.73	3.64	19.96	99.8	1.27	6.36
10	10.57	105.7	0.94	8.52	11.03	110.3	0.48	4.34

[a]Assay was completed every 3 d for 15 d continuously. [b]Mean value of 5 replicates at each spiked concentration.

In addition, pH value, methanol content of the sample extract, and interpretation time could influence the sensitivity and reproducibility of the QB-ICA sensor. In the present study, immunological kinetics analysis was introduced to elaborate the effects of the above factors according to our previous works.[31] The kinetic curves between QB-mAbs and AFB_1–BSA on the test line, as well as those of the QB-mAbs and donkey anti-mouse antibody on the control line, were established by plotting the development of FI_T, FI_C, and FI_T/FI_C against immunoreaction time. Figure 3A (inset) shows the results, indicating that the FIs on both lines enhance continuously during the 45 min observation period. However, FI_T/FI_C reached a constant value after 15 min, even with higher AFB_1 concentration (Figure 3A). These results indicated that FI_T/FI_C could shorten the interpretation time of the ICA sensor, and the 15 min immunoreaction time was necessary for ICA quantitative analysis. To explore the effects of pH on FI_T, FI_C, and FI_T/FI_C, we adjusted the pH values of the sample solutions to final pH values of 5.0, 6.0, 7.0, 8.0, and 9.0 and then tested the samples with a QB-ICA sensor. For the AFB_1 negative sample, FI_T improved sharply, when pH increased from 5.0 to 7.0, and then reached a relatively stable level between 971.45 and 1088.88, with the pH ranging from 7.0 to 9.0. Meanwhile, FI_C decreased as pH increased (Figure 3B). However, the competitive inhibition rates for AFB_1 concentration at 10 pg mL^{-1} were relatively constant between 37.52 and 41.16%, and the pH values ranged from 5.0 to 9.0. To obtain a strong fluorescence signal on the test line, we selected 0.01 M PBS with a pH of 7.4 as the optimal pH condition for all succeeding experiments.

Higher extraction recovery from AFB_1 polluted real samples requires the extract solution to contain a certain concentration of methanol because of the hydrophobic property of AFB_1. In this study, the effects of methanol on FI_T, FI_C, FI_T/FI_C, and competitive inhibition were investigated. The results shown in Figure 3D indicate that the competitive inhibition rate declines from 41.97 to 40.24% when methanol content is lower than 5%, and declines sharply to 12.37% when methanol content increases to 40%. Considering the ultrasensitivity of the proposed method, the real sample extract should be diluted with 0.01 M PBS (pH 7.4) to obtain a final methanol concentration of 3% for all subsequent experiments.

3.4. Analytical Performance of the QB-ICA Sensor. Under optimal experimental conditions, the calibration curve of the QB-ICA sensor was constructed by plotting the $B/B_0 \times 100\%$ against the logarithm of various concentrations of the AFB_1 analytical standard (0–200 pg mL^{-1}). Figure 3C shows the calibration curve exhibiting a good linear range from 5 to 60 pg mL^{-1} with a reliable correlation coefficient ($R^2 = 0.99$). The regression equation could be represented by $y = (0.28 \ln x) + 1.25$, where y is the competitive inhibition rate and x is the AFB_1 concentration. Error bars were based on three duplicate measurements at different AFB_1 concentrations. The IC_{50} of the QB-ICA sensor was achieved at 13.87 ± 1.54 pg mL^{-1} (n = 3), which is significantly lower (39-fold) than that of the QDs as a signal probe (IC_{50} = 0.54 ± 0.06 ng mL^{-1}; Figure S7, Supporting Information). The LOD was calculated at 0.42 pg mL^{-1} according to the mean plus 3 times standard deviation (SD),[32,33] which corresponds to 1.34 fmol of analyte in a 1 mL sample solution. The mean and SD were obtained by applying 20 duplicate measurements of the blank sample. Such a high LOD highlights that the QBs have an important role for signal amplification probes in QB-ICA sensor.

The specificity of the QB-ICA sensor was evaluated by running four structurally related analogs (AFG_1, AFG_2, AFM_1, and AFB_2) and other five common mycotoxins (citrinin, patulin, ochratoxin A, deoxynivalenol, and zearalenone). The cross-reaction (CR) was calculated according to the following equation: $CR\ \% = [(IC_{50\ AFB1})/(IC_{50\ analog})] \times 100$.[34] The results show that the developed method exhibited 51.6, 0.2, 1.73, and 5.58% CR to AFG_1, AFG_2, AFM_1, and AFB_2, respectively, and negligible (<0.01%) CR to the other five mycotoxins.

Recovery studies of the intra- and inter-assay were conducted to evaluate the accuracy and precision of the proposed method by analyzing three spiked maize extracts with low (10 pg mL^{-1}), medium (20 pg mL^{-1}), and high (40 pg mL^{-1}) levels of AFB_1 concentrations. The intra-assay was completed within 1 d with five replicates at each spiked concentration, and the inter-assay was completed every 3 d for 15 d continuously with five replicates at each spiked concentration. Table 1 shows the results. The average recoveries for the intra-assay ranged from 97.89 to 105.70%, with a CV ranging from 3.64 to 8.52%. The results for the inter-assay ranged from 96.32 to 110.30% and 4.34 to 6.36%, respectively. The variations for intra- and inter-assay using QB-ICA sensor are acceptable levels for AFB_1 quantitative analysis.[35,36]

3.5. Determination of AFB_1 in the Real Samples. The acceptance of the new QB-ICA sensor for AFB_1 was compared with a commercial ELISA kit by blindly analyzing 40 AFB_1 spiked real maize samples. The results (Figure 4) show that the two methods exhibited good agreement with a highly significant correlation (R^2 = 0.93). The proposed QB-ICA sensor took only 15 min to complete one sample analysis, whereas traditional ELISA took 90 min. To further demonstrate the reliability and practicability of the proposed QB-ICA sensor in real samples, different feedstuffs, including maize, soybean meal, rapeseed meal, cotton seed meal, distillers dried grain, and wheat sample, were analyzed using QB-ICA sensor and liquid chromatography-tandem mass spectrometry (LC–MS/MS). The results in Table 2 show that four samples were found with AFB_1 contamination by both methods, and the established QB-ICA method did not show any false-negative or false-positive result.

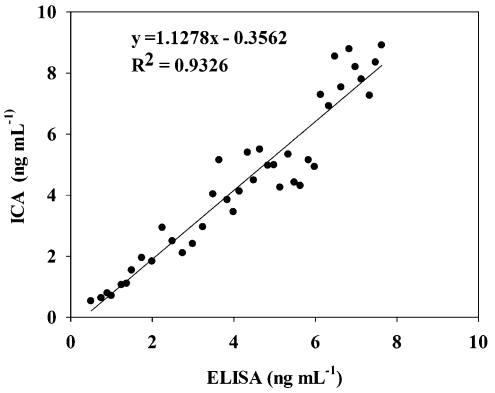

Figure 4. Correlation between results from (x axis) ELISA and QB-ICA (y axis) sensor analyses of AFB_1 in 40 spiked samples. Blank samples were spiked with different concentrations (from 0.5 to 9 ng) of AFB_1 standard solutions.

Table 2. Determination of AFB_1 Pollution in Real Feedstuff Materials with LC−MS/MS and QB-ICA Sensor

feedstuff materials	LC−MS/MS (ng g^{-1})[a]	strip (ng g^{-1})[a]
maize no. 1	–[b]	–
maize no. 2	31.70 ± 3.02	36.98 ± 3.27
maize no. 3	1.35 ± 0.15	1.61 ± 0.14
maize no. 4	–	–
cottonseed meal	198.38 ± 9.61	172.00 ± 7.89
soybean meal	1.91 ± 0.16	2.26 ± 0.20
wheat	–	–
rapeseed meal	–	–
distillers dried grain	–	–

[a]Mean of three determinations ± SD. [b]–, not detected.

4. CONCLUSIONS

Highly luminescent submicrobeads were successfully prepared with embedding assembly technology. The submicrobeads exhibited approximately 2863 times higher luminescence intensity than the corresponding CdSe/ZnS QDs. This highly luminescent amplification probe, with numerous QDs instead of a single QD contained in each antigen−antibody interaction event, demonstrated that the detectable signal is dramatically amplified, as expected. The numerous QDs and their unique properties made the QBs a potential amplified label for application in bioanalysis. An immunochromatrographic strip sensor based on QBs as reporters was constructed to evaluate their practicability. With the incorporation of the advantages of the immunochromatrographic strip sensor, a simple method for rapid screening of AFB_1 in maize with superior performance is obtained, using functionalized QBs as a carrier-amplified label. Under optimal conditions, the LOD reached 0.42 pg mL^{-1}, which corresponded to 1.34 fmol of the target AFB_1 in 1 mL sample solution. The CVs for intra- and inter-assay were below 10%. The recoveries obtained from the QB-ICA sensor ranged from 71.39% to 128.62%, which were comparable with those obtained from a commercial ELISA kit, with a highly significant correlation (R^2 = 0.93). The feasibility of the proposed method for detection of other grain samples was also confirmed by LC−MS/MS method. Our proposed method could provide promising and versatile opportunities for the rapid screening of other toxins at ultrasensitive levels in agricultural products and foods by combining the carrier-amplified label with the ICA sensor.

ASSOCIATED CONTENT

Supporting Information

Absorption and fluorescence spectra of CdSe/ZnS QDs; histogram of size distribution of QBs; fluorescence spectra of QDs and the prepared QBs; determination of the amounts of the target antibody in ascites; confirmation of the saturation concentration of the ascites conjugated with the QBs; optimization of the QBs strip parameters; the stereogram of the strip, the standard curve of the QD-based ICA sensor and the consumption of antibodies between QB-ICA and QD-ICA sensor. This material is available free of charge via the Internet at http://pubs.acs.org.

AUTHOR INFORMATION

Corresponding Authors

*Phone: +0086-791-8833-4578. Fax: +0086-791-8833-3708. E-mail: yhxiongchen@163.com. Address: 235 Nanjing E. Road, Nanchang 330047, People's Republic of China.
*Phone: +001-858-689-8808. E-mail: nanoio2010@gmail.com.

Author Contributions

‖These authors contributed equally to this work.

Notes

The authors declare no competing financial interest.

ACKNOWLEDGMENTS

This work was supported by a grant from the National Basic Research Program of China (2013CB127804), the Twelfth Five-Year Plan for National Science and Technology Support Program (2013BAD19B02 and 2012BAK17B02), the Research Program of the State Key Laboratory of Food Science and Technology, Nanchang University (SKLF-ZZB-201306), the Training Plan for the Main Subject of Academic Leaders of Jiangxi Province (20142BCB22004), and the National Institute of Health of the United States (1R43AI092962).

REFERENCES

(1) Guo, X.; Wen, F.; Zheng, N.; Luo, Q.; Wang, H.; Wang, H.; Li, S.; Wang, J. Development of an Ultrasensitive Aptasensor for the Detection of Aflatoxin B1. *Biosens. Bioelectron.* **2014**, *56*, 340−344.
(2) Xu, X.; Liu, X.; Li, Y.; Ying, Y. A Simple and Rapid Optical Biosensor for Detection of Aflatoxin B1 Based on Competitive Dispersion of Gold Nanorods. *Biosens. Bioelectron.* **2013**, *47*, 361−367.
(3) Zhang, X.; Feng, M.; Liu, L.; Xing, C.; Kuang, H.; Peng, C.; Wang, L.; Xu, C. Detection of Aflatoxins in Tea Samples Based on a Class-Specific Monoclonal Antibody. *Int. J. Food Sci. Technol.* **2013**, *48*, 1269−1274.
(4) Fang, L.; Chen, H.; Ying, X.; Lin, J. M. Micro-Plate Chemiluminescence Enzyme Immunoassay for Aflatoxin B1 in Agricultural Products. *Talanta* **2011**, *84*, 216−222.
(5) Xu, K.; Sun, Y.; Li, W.; Xu, J.; Cao, B.; Jiang, Y.; Zheng, T.; Li, J.; Pan, D. Multiplex Chemiluminescent Immunoassay for Screening of Mycotoxins Using Photonic Crystal Microsphere Suspension Array. *Analyst (Cambridge, U.K.)* **2014**, *139*, 771−777.
(6) Yu, F. Y.; Gribas, A. V.; Vdovenko, M. M.; Sakharov, I. Y. Development of Ultrasensitive Direct Chemiluminescent Enzyme Immunoassay for Determination of Aflatoxin B1 in Food Products. *Talanta* **2013**, *107*, 25−29.
(7) Hu, W.; Li, X.; He, G.; Zhang, Z.; Zheng, X.; Li, P.; Li, C. M. Sensitive Competitive Immunoassay of Multiple Mycotoxins with Non-Fouling Antigen Microarray. *Biosens. Bioelectron.* **2013**, *50*, 338−344.
(8) Deng, G.; Xu, K.; Sun, Y.; Chen, Y.; Zheng, T.; Li, J. High Sensitive Immunoassay for Multiplex Mycotoxin Detection with

Photonic Crystal Microsphere Suspension Array. *Anal. Chem.* **2013**, *85*, 2833−2840.
(9) Pribul, V.; Woolley, T. Point of Care Testing. *Surgery (Oxford)* **2013**, *31*, 84−86.
(10) Li, X.; Li, P.; Zhang, Q.; Li, R.; Zhang, W.; Zhang, Z.; Ding, X.; Tang, X. Multi-Component Immunochromatographic Assay for Simultaneous Detection of Aflatoxin B1, Ochratoxin A, and Zearalenone in Agro-Food. *Biosens. Bioelectron.* **2013**, *49*, 426−432.
(11) Moon, J.; Kim, G.; Lee, S. A Gold Nanoparticle and Aflatoxin B1-BSA Conjugates Based Lateral Flow Assay Method for the Analysis of Aflatoxin B1. *Materials* **2012**, *5*, 634−643.
(12) Zhang, D.; Li, P.; Yang, Y.; Zhang, Q.; Zhang, W.; Xiao, Z.; Ding, X. A High Selective Immunochromatographic Assay for Rapid Detection of Aflatoxin B1. *Talanta* **2011**, *85*, 736−742.
(13) Anfossi, L.; D'Arco, G.; Calderara, M.; Baggiani, C.; Giovannoli, C.; Giraudi, G. Development of a Quantitative Lateral Flow Immunoassay for the Detection of Aflatoxins in Maize. *Food Addit. Contam., Part A* **2011**, *28*, 226−234.
(14) Zhang, D. H.; Li, P. W.; Zhang, Q.; Zhang, W. Ultrasensitive Nanogold Probe-Based Immunochromatographic Assay for Simultaneous Detection of Total Aflatoxins in Peanuts. *Biosens. Bioelectron.* **2011**, *26*, 2877−2882.
(15) Blažková, M.; Javůrková, B.; Fukal, L.; Rauch, P. Immunochromatographic Strip Test for Detection of Genus *Cronobacter*. *Biosens. Bioelectron.* **2011**, *26*, 2828−2834.
(16) Liu, C.; Jia, Q.; Yang, C.; Qiao, R.; Jing, L.; Wang, L.; Xu, C.; Gao, M. Lateral Flow Immunochromatographic Assay for Sensitive Pesticide Detection by Using Fe_3O_4 Nanoparticle Aggregates as Color Reagents. *Anal. Chem.* **2011**, *83*, 6778−6784.
(17) Corstjens, P. L.; de Dood, C. J.; van der Ploeg-van Schip, J. J.; Wiesmeijer, K. C.; Riuttamäki, T.; van Meijgaarden, K. E.; Spencer, J. S.; Tanke, H. J.; Ottenhoff, T. H.; Geluk, A. Lateral Flow Assay for Simultaneous Detection of Cellular and Humoral Immune Responses. *Clin. Biochem.* **2011**, *44*, 1241−1246.
(18) Song, X.; Knotts, M. Time-Resolved Luminescent Lateral Flow Assay Technology. *Anal. Chim. Acta* **2008**, *626*, 186−192.
(19) Yang, Q.; Gong, X.; Song, T.; Yang, J.; Zhu, S.; Li, Y.; Cui, Y.; Li, Y.; Zhang, B.; Chang, J. Quantum Dot-Based Immunochromatography Test Strip For Rapid, Quantitative, and Sensitive Detection of Alpha Fetoprotein. *Biosens. Bioelectron.* **2011**, *30*, 145−150.
(20) Yan, J.; Estévez, M. C.; Smith, J. E.; Wang, K.; He, X.; Wang, L.; Tan, W. Dye-Doped Nanoparticles for Bioanalysis. *Nano Today* **2007**, *2*, 44−50.
(21) Michalet, X.; Pinaud, F.; Bentolila, L.; Tsay, J.; Doose, S.; Li, J.; Sundaresan, G.; Wu, A.; Gambhir, S.; Weiss, S. Quantum Dots for Live Cells, in Vivo Imaging, and Diagnostics. *Science* **2005**, *307*, 538−544.
(22) Resch-Genger, U.; Grabolle, M.; Cavaliere-Jaricot, S.; Nitschke, R.; Nann, T. Quantum Dots versus Organic Dyes As Fluorescent Labels. *Nat. Methods* **2008**, *5*, 763−775.
(23) Zhang, P.; Lu, H.; Chen, J.; Han, H.; Ma, W. Simple and Sensitive Detection of HBsAg by Using a Quantum Dots Nanobeads Based Dot-Blot Immunoassay. *Theranostics* **2014**, *4*, 307−315.
(24) Xiang, Y.; Zhang, H.; Jiang, B.; Chai, Y.; Yuan, R. Quantum Dot Layer-by-Layer Assemblies as Signal Amplification Labels for Ultrasensitive Electronic Detection of Uropathogens. *Anal. Chem.* **2011**, *83*, 4302−4306.
(25) Li, X.; Li, W.; Yang, Q.; Gong, X.; Guo, W.; Dong, C.; Liu, J.; Xuan, L.; Chang, J. Rapid and Quantitative Detection of Prostate Specific Antigen with a Quantum Dot Nanobeads-Based Immunochromatography Test Strip. *ACS Appl. Mater. Interfaces* **2014**, *6*, 6406−6414.
(26) Xie, R.; Kolb, U.; Li, J.; Basché, T.; Mews, A. Synthesis and Characterization of Highly Luminescent CdSe-Core $CdS/Zn_{0.5}Cd_{0.5}S$/ZnS Multishell Nanocrystals. *J. Am. Chem. Soc.* **2005**, *127*, 7480−7488.
(27) Mendes, R.; Carvalhal, R.; Stach-Machado, D.; Kubota, L. Surface Plasmon Resonance Immunosensor for Early Diagnosis of Asian Rust on Soybean Leaves. *Biosens. Bioelectron* **2009**, *24*, 2483−2487.
(28) Kim, H. K.; Kang, S. J.; Choi, S. K.; Min, Y. H.; Yoon, C. S. Highly Efficient Organic/Inorganic Hybrid Nonlinear Optic Materials via Sol-Gel Process: Synthesis, Optical Properties, and Photobleaching for Channel Waveguides. *Chem. Mater.* **1999**, *11*, 779−788.
(29) Chen, X. L.; Xu, H. Y.; Lai, W. H.; Chen, Y.; Yang, X. H.; Xiong, Y. H. A Sensitive Chromatographic Strip Test for the Rapid Detection of Enrofloxacin in Chicken Muscle. *Food Addit. Contam., Part A* **2012**, *29*, 383−391.
(30) Molinelli, A.; Grossalber, K.; Krska, R. A Rapid Lateral Flow Test for the Determination of Total Type B Fumonisins in Maize. *Anal. Bioanal. Chem.* **2009**, *395*, 1309−1316.
(31) Huang, X.; Aguilar, Z. P.; Li, H.; Lai, W.; Wei, H.; Xu, H.; Xiong, Y. Fluorescent $Ru(phen)_3^{2+}$-Doped Silica Nanoparticles-Based ICTS Sensor for Quantitative Detection of Enrofloxacin Residues in Chicken Meat. *Anal. Chem.* **2013**, *85*, 5120−5128.
(32) Oh, S. W.; Kim, Y. M.; Kim, H. J.; Kim, S. J.; Cho, J. S.; Choi, E. Y. Point-of-Care Fluorescence Immunoassay for Prostate Specific Antigen. *Clin. Chim. Acta* **2009**, *406*, 18−22.
(33) Pleadin, J.; Vulić, A.; Perši, N.; Vahčić, N. Clenbuterol Residues in Pig Muscle after Repeat Administration in a Growth-Promoting Dose. *Meat Sci.* **2010**, *86*, 733−737.
(34) Li, C.; Luo, W.; Xu, H.; Zhang, Q.; Xu, H.; Aguilar, Z. P.; Lai, W.; Wei, H.; Xiong, Y. Development of an Immunochromatographic Assay for Rapid and Quantitative Detection of Clenbuterol in Swine Urine. *Food Control* **2013**, *34*, 725−732.
(35) Semenova, V.; Schiffer, J.; Steward-Clark, E.; Soroka, S.; Schmidt, D.; Brawner, M.; Lyde, F.; Thompson, R.; Brown, N.; Foster, L. Validation and Long Term Performance Characteristics of a Quantitative Enzyme Linked Immunosorbent Assay (ELISA) for Human Anti-PA IgG. *J. Immunol. Methods* **2012**, *376*, 97−107.
(36) Bai, Y.; Liu, Z.; Bi, Y.; Wang, X.; Jin, Y.; Sun, L.; Wang, H.; Zhang, C.; Xu, S. Preparation of Polyclonal Antibodies and Development of a Direct Competitive Enzyme-Linked Immunosorbent Assay to Detect Residues of Phenylethanolamine A in Urine Samples. *J. Agric. Food Chem.* **2012**, *60*, 11618−11624.